Title	Incorporation of the effect of the composite electric fields of molecular ions as a simulation tool for biological damage due to heavy-ion irradiation
Author(s)	Kengo Moribayashi
Citation	Physical Review A,84(1):012702
Text Version	Publisher
URL	http://jolissrch-inter.tokai-sc.jaea.go.jp/search/servlet/search?5028888
DOI	http://dx.doi.org/10.1103/PhysRevA.84.012702
Right	© 2011 The American Physical Society

Incorporation of the effect of the composite electric fields of molecular ions as a simulation tool for biological damage due to heavy-ion irradiation

Kengo Moribayashi*

Quantum Beam Science Directorate, Japan Atomic Energy Agency, 8-1-7 Umemidai, Kizugawa-City, Kyoto 619-0215, Japan and Faculty of Life and Medical Sciences, Doshisha University, 1-3 Tatara Miyakodani, Kyotanabe City, Kyoto 610-0394, Japan

(Received 1 December 2010; published 7 July 2011)

This paper presents a theoretical study of the DNA damage due to the effect of the composite electric fields of H_2O^+ ions produced from the irradiation of a heavy ion onto a cell. A model for atomic and molecular processes in strong electric fields is developed. It is found that the composite electric fields increase the number of events of electron-impact ionization processes. This may promote DNA damage.

DOI: 10.1103/PhysRevA.84.012702 PACS number(s): 34.90.+q, 34.10.+x, 36.40.Gk

I. INTRODUCTION

Swift heavy ions are a good research tool in the fields of biological physics [1,2], surface science [3–5], and medical science [6–8]. For example, in biological physics, although there are several hypotheses, the important phenomenon of relative biological effectiveness (RBE) is not yet fully understood, and one might ask why do heavier ions produce more cluster DNA damage [9,10] and lead to high RBE values. The understanding of RBE is directly connected to the understanding of the reason why cancer therapy using C^{6+} ions has a higher efficiency than that using protons [11]. In this paper, we propose and quantify an explanation for RBE that hinges on the effect of the composite electric fields of molecular ions (mainly H_2O^+), which are produced by heavy-ion-impact ionization processes, in a cell by comparing the irradiation of a C^{6+} ion with that of a proton onto the cell.

The stronger composite electric fields are formed as cross sections of the incident ion-impact ionization process become larger. This comes from the following. The molecules in the cell on the track of the incident ion are ionized according to the impact ionization cross sections of the incident ion. Larger cross sections of incident ion-impact ionization produce a shorter average interval length between molecular ions in the cell because the mean path between ionization events can be expressed by multiplication of the cross section of the ion-impact ionization and the density of molecules. Then, a stronger composite electric field is formed from the shorter average interval length between molecular ions. For example, for the irradiation of C^{6+} ions with the energy of a few MeV/u, we estimate the mean path between ionization events at about 0.3 nm, which is almost as large as the average interval lengths between molecules in a cell, using C^{6+} ion-impact ionization cross sections [12] and the density of the molecules in a cell. Then, almost all of the molecules on the track of the incident ion are ionized, and strong composite electric fields may be formed near the track. On the other hand, we estimate the interval length between molecular ions at about 0.8 nm in the case of the irradiation of protons with the energy of a few 100 keV/u where the impact ionization cross section becomes a maximum as a function of energy of the protons [13]. We have found that the composite electric fields formed from the irradiation of C^{6+} ions with the energy of a few MeV/u are stronger than those from the irradiation of protons. Simulation results show the same tendency for the relationship between the cross sections of the incident ion-impact ionization and the formation of the composite electric field (see Sec. IV A and Figs. 2 and 3).

Electrons, which are produced from impact ionization processes of an incident ion or electrons, play an important role in the DNA damage. The composite electric fields may trap the electrons near the track of the incident ion. Then, the electrons near the track may be able to continue to have enough energy to ionize the molecules through electron-impact ionization because of strong electric fields. We expect that the number of electrons produced here, by including the effect of the composite electron fields, becomes larger than that by excluding this effect. Our simulation results become just what we have expected here (see Sec. IV C). Also, it should be noted that the electrons produced near the track may often produce cluster DNA damage [9,10], which may play an important role in RBE because the cluster DNA damage is apt to be produced near the track.

This paper develops a model in atomic and molecular processes in electric fields and tells us how plasmas are produced due to heavy-ion irradiation onto matter (see Secs. III C and IV C).

The increase in the cross sections of the ion-impact ionization produces a stronger effect of the composite electric field. These cross sections become larger according to the increase in the charge of the incident ion. The effect of the composite electric field may play an important role in the research of the damage on human bodies or semiconductors [3] in the space environment because a lot of highly charged ions, such as Fe^{26+} exist there.

II. THE CONTENTS OF SIMULATIONS

We treat a C^{6+} ion with the energy from a few MeV/u to 100 MeV/u and a proton with that from a few 100 keV/u to 1 MeV/u as an incident ion and H_2O molecules as a component of the target because H_2O is the main component in cells. We calculate (i) the generation of H_2O^+ ions, electrons, and the excited states of H_2O due to the impact processes of the incident ion or electrons. (The details and the simulation methods are presented in the subsection in

*moribayashi.kengo@jaea.go.jp

Secs. II and III B–III D, respectively) and (ii) the movement of the electrons in the electric field formed by the ions and electrons (the simulation methods are presented in Sec. III E). It should be noted that, in our model, the composite electric fields are included in the movement of electrons by treating the interaction of the electron of interest with all of the H_2O^+ ions and the other electrons.

We ignore the movement of H_2O^+ ions in our simulation for the following reasons. Even when almost all of the atoms in the proteins are ionized by the irradiation of high-intensity x rays, Hau-Riege *et al.* [14] showed, from their simulation, that the water molecules surrounding the protein can control the movement of atoms so that they move little during time scales smaller than 50 fs [14]. In the irradiation of a heavy ion onto a cell, the number of surrounding water molecules is much larger, and the number of ions, which surround the H_2O^+ ion of interest, is smaller resulting in a smaller Coulomb force acting on each ion.

A. Atomic and molecular processes

After an incident ion (A^{z+}) enters the target, we consider the following atomic and molecular processes. (i) The incident ion interacts with an H_2O molecule, then, an electron is emitted through ion-impact ionization processes ($A^{z+} + H_2O \rightarrow A^{z+} + H_2O^+ + e^-$). (ii) The electrons emitted here also interact with H_2O molecules, then ionization ($e^- + H_2O \rightarrow e^- + H_2O^+ + e^-$), electronic and vibrational excitation ($e^- + H_2O \rightarrow e^- + H_2O^*$) processes occur, where H_2O and H_2O^* are the ground state and the excited states of a water molecule, respectively. (iii) Electrons are emitted from the electronic excited state due to electron impact ($e^- + H_2O^* \rightarrow e^- + H_2O^+ + e^-$). This comes from the fact that cross sections of the electron-impact excitation processes are much larger than those of the electron-impact ionization at the energies of electrons from 10 to 20 eV [15,16]. In this energy range, the population of electrons becomes the largest at times greater than a few femtoseconds after the incident ion enters the target. It is expected that a lot of electronic excited states of H_2O may be produced. It should be noted that we do not need to consider this process in the case without the electric field because the interaction time is so small that electrons have seldom collided with the electronic excited state of H_2O.

The charge of the incident ion changes [13,17–19] during the movement of the incident ion in the target. However, we do not change the charge in our simulation for the following reasons. As for the irradiation of a C^{6+} ion at the energy of 3 MeV/u, one or no electron is captured, then, the probability (P_e) of the existence of C^{6+} is determined by

$$P_e \sim \frac{\sigma_{el}}{\sigma_{ct} + \sigma_{el}}, \tag{1}$$

where σ_{ct} and σ_{el} are cross sections of the charge transfer ($C^{6+} + H_2O \rightarrow C^{5+} + H_2O^+$) and the electron loss ($C^{5+} + H_2O \rightarrow C^{6+} + H_2O + e^-$), respectively [13,18]. Since the charge- transfer and electron-loss cross sections roughly increase according to Z^3 and decrease according to Z^{-2}, respectively [19,20], we roughly estimate $\sigma_{ct} \sim 5 \times 10^{-19}$ cm^2 and $\sigma_{el} \sim 2 \times 10^{-18}$ cm^2 from the cross sections of He^{2+} and He^+, respectively [18], where Z is the charge of the ion. Therefore, the existence probability of C^{6+} is about 80%. Even the impact ionization cross section of C^{5+} ions at 3 MeV/u is about 10^{-15} cm^2 [12,19]. This cross section satisfies the condition that the mean path between ionization events is almost as large as the average interval length between H_2O molecules in a cell. It should be noted that, as soon as the charge of carbon ions becomes smaller than 4, electron-loss processes occur, and the charge increases. Therefore, we ignore the charge smaller than 4. As for the irradiation of a proton, there is little difference between the cross sections of impact ionization of protons and hydrogen atoms at the energy of a few 100 keV/u [13].

III. SIMULATION METHODS

A. Setup of target and incident ions

We consider a rectangular volume with the size of 10 nm × 10 nm (area of the bottom or the top) × 20 nm (height) as a target. In the target, we arrange H_2O molecules as the density of molecules becomes that of a liquid. Then, the places of the molecules are assigned randomly on the condition that they are located inside the target and that lengths between the molecules are larger than 2.7 Å. The incident ion enters the target from the center of the bottom area of the target and moves perpendicular to the bottom area of the target. We assume that the energy and the movement direction of the C^{6+} ion or the proton do not change during the movement in the target because the size of the target is so small that there is little change.

B. The particle-impact processes

We calculate the change of electronic states of H_2O in the target according to the particle- (the electron- or the ion-) impact processes as a function of time. Since we treat the particles individually, we employ the same method as that employed in molecular dynamic (MD) simulation [21] for the treatment of the particle-impact processes using the cross sections as follows. The center of the cross section is located at the center of the atom or the molecule (H_2O in this paper), and the cross section is perpendicular to the direction of the velocity of the particle. It is judged that the particle-impact process occurs only when the particle crosses the area of its corresponding cross section [21–23]. Specifically, we use the relationship of cross sections with impact parameters (b) where b is defined as the perpendicular distance between the path of an incident ion and the center of the molecule (H_2O). The particle-impact cross section (σ) is given by

$$\sigma = \pi \int_0^{b_{\max}} p(b)\, b\, db, \tag{2}$$

where $P(b)$ is the probability that the corresponding processes occur as a function of b and $b_{\max}$ is the maximum b where the process occurs. When we assume $P(b)$ to be a step function with value 0 outside of $b_{\max}$, $\sigma = \pi b_{\max}^2$. Only when b becomes smaller than $(\sigma/\pi)^{1/2}$, do we judge that the particle-impact process occurs. However, $P(b)$ is not a step function. When we treat $P(b)$ exactly, the track may be thicker. Then, stronger composite electric fields may be produced. Therefore, we will treat $P(b)$ exactly in the future. We use the total cross sections

for all the possible transitions. The process is chosen randomly among them using the respective cross sections as weighting factors.

Since particle-impact cross sections used here differ from the definition, we checked this by treating the particle-impact processes correctly in our previous paper [24] where we studied the irradiation of high-intensity x rays onto a cluster or a biomolecule. We showed good agreement of the frequencies of electron-impact ionization processes calculated by the method treated here with those by rate equations. In the rate equations [25–27], the electron-impact ionization cross sections are treated as a probability that the corresponding processes occur. Then, the rates of the electron-impact ionization processes (R_{ei}) are given by

$$R_{ei} = N_e \sigma_{ei} v_e, \tag{3}$$

where N_e, σ_{ei}, and v_e are the electron density, the cross sections of the electron-impact ionization process, and the velocity of the electron, respectively.

If we consider cross sections including the effect of the electric field, the cross sections become larger. Therefore, the effect of the composite electric fields may be larger than that treated in this paper.

C. Initial electron energies

Electrons are generated from the particle-impact ionization processes. The DNA damage depends on the generated electron number and energies. Here, we mention the initial electron energies. It should be noted that there is a difference between the initial energies of the electrons including and excluding electric fields in the simulation models. Figure 1 shows the potential energy curve [$V(r)$] inside an atom or a molecule including and excluding the electric field as a function of r, where B, E_i , r, and r_0 are the binding energy of H_2O, the experimental data for the initial energy of electrons

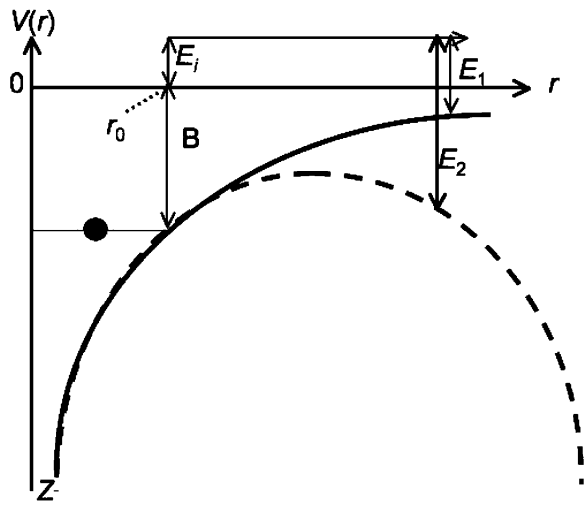

FIG. 1. The relationship of the potential energy curves [$V(r)$] given in an atom (or a molecule) as a function of r including (broken line) and excluding (solid line) composite electric fields of H_2O^+ ions with energies (B, E_i, E_1, E_2) relevant to an electron emitted as explained in the text.

emitted from H_2O, the radii from the center of this parent molecule, and the place where the electron is emitted from this parent molecule, respectively. We take $r = 0$ at the center of the atom or the molecule. In the case including the electric field, we take r to be in the direction of the track of the incident ion. We estimate E_i for ion- and electron-impact ionization processes according to the formula given by Rudd *et al.* [28] and Nakazaki *et al.* [29], respectively. However, the real initial energy of the electron is not E_i but $E_i + B$ according to energy conservation. When we do not consider electric fields, we have to use E_i as an initial energy. This treatment is not bad because E_1 becomes E_i soon after the electron leaves the parent molecule as seen in Fig. 1, where E_1 is the energy of the electron at r in the case without electric fields. However, we must use $(E_i + B)$ as an initial energy in the existence of strong electric fields because E_2 is often much larger than E_i, where E_2 is the electron energy in the electric field.

D. Data for cross sections and initial electron energies treated here

In order to treat particle-impact processes, we employ the available data for the cross sections and initial electron energies as follows. (i) For impact ionization processes of protons and C^{6+} ions, we employ the cross sections as a function of energy of the incident ion given by Uehara *et al.* [13] and Cappello *et al.* [12], respectively. Then, the value of E_i (see Sec. III C and Fig. 1) emitted here is determined randomly by treating the energy distribution estimated from the Rudd model [28] as weighting factors, and the incident angle is also determined randomly. (ii) For the electron-impact ionization, electronic, and vibrational excitation, we use the cross sections given by Orient and Srivastava [15], Pritchard *et al.* [16], and Nishimura and Itikawa [30], respectively. (iii) The cross sections of electron-impact ionization from the excited state (σ_{ie}) are much larger than those from the ground state (σ_{ig}) [15]. Here, $\sigma_i e$ is roughly estimated from σ_{ig} and the formula given by Lotz [31], that is,

$$\sigma_{ie}(E_e) \alpha \sigma_{ig}(E_e{}') \frac{B_{ig} E_e \ln(E_e{}'/B_{ie})}{B_{ie} E_e{}' \ln(E_e/B_{ig})}, \tag{4}$$

where E_e, B_{ig}, and B_{ie} are the incident electron energy, the bound energy from the ground state, and that from the excited state of H_2O, respectively. The value of E_i and the angle of the electron emitted here by the electron-impact ionization are determined by the data given by Nakazaki *et al.* [29] and random numbers, respectively. It should be noted that we need to add B to E_i to determine the initial electron energy as mentioned in Sec. III C.

E. The movement of the electrons

The Coulomb forces due to ions and electrons act on the electrons. The movement of these electrons is solved by Newton's equations, that is,

$$\vec{F} = m_e \frac{d\vec{v}_{ei}}{dt} = -\sum_{j \neq i} \frac{e^2 \vec{r}_{ij}}{4\pi\varepsilon_0 r_{ij}^3} + \sum_l \frac{q_l e \vec{r}_{il}}{4\pi\varepsilon_0 r_{il}^3}, \tag{5}$$

where ϵ_0, m_e, $\vec{v}_{ei}$, q_l, and $\vec{r}_{ij(l)}$ are the dielectric constant in vacuum, the mass of an electron, the velocity of the ith electron, the charge of the lth ion, and the distances between the ith electron and the jth electron (the lth ion), respectively [22,23]. In order to avoid the divergence near $\vec{r}_{ij(l)} = 0$ in Eq. (5), we use a similar approximation as that employed in MD simulation [21], that is, $\vec{r}_{ij(l)}$ is approximately replaced by $(r_{ij(l)}^2 + a_s^2)^{1/2}$, where we take a_s to be 0.1 nm [22,23].

We assume that the electric field varies periodically along the z axis because the interval length between H_2O^+ ions produced from heavy-ion-impact ionization is almost a constant value. Then, we move the electrons that leave the bottom or top area of the target to the top or bottom area, respectively.

IV. RESULTS AND DISCUSSIONS

A. Formation of composite electric field

Figure 2 shows examples of the places where H_2O^+ ions are produced by the incident ion-impact ionization cross sections of 1.5×10^{-15}, 4×10^{-16}, 2×10^{-16}, and 10^{-16} cm^2. The cross sections of 1.5×10^{-15}, 4×10^{-16}, 2×10^{-16}, and 10^{-16} cm^2 correspond to the incident ions of C^{6+} ions with the energy of 3 MeV/u, C^{6+} ions with the energy of 15 MeV/u or protons

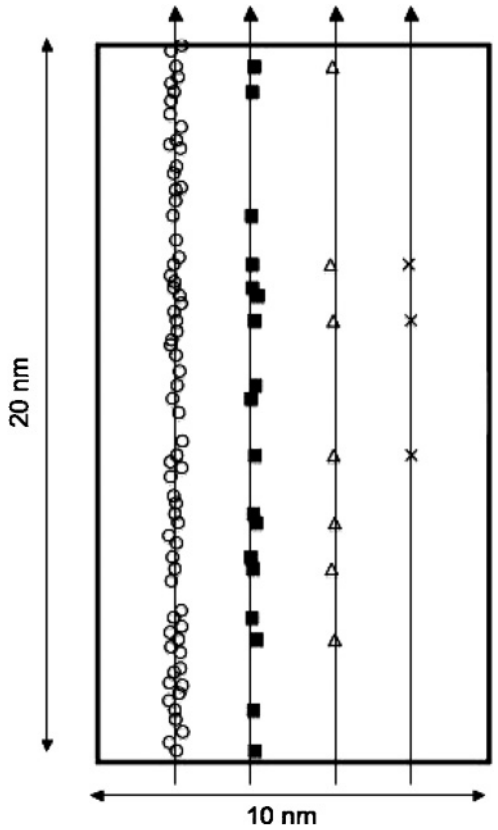

FIG. 2. Examples of the places where H_2O^+ ions are produced near the track of ions with the ion-impact ionization cross sections of 1.5×10^{-15} (◯), 4×10^{-16} (■), 2×10^{-16} (△), and 10^{-16} cm^2 (×). The arrows express the direction of the motion of the ions. The lengths of the targets are 20 (the direction of the track of the incident ions) and 10 nm (the direction that is perpendicular to the track).

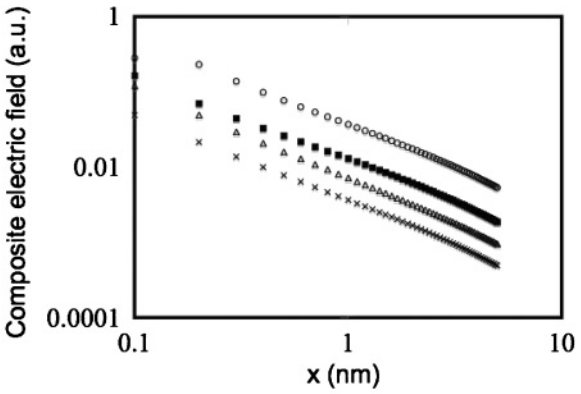

FIG. 3. Composite electric fields on the x axis vs x. The impact ionization cross sections are 1.5×10^{-15} (◯), 4×10^{-16} (■), 2×10^{-16} (△), and the proton and 10^{-16} cm^2 (×). The electric field of 1 a.u. corresponds to about 5×10^{11} V/m.

with the energy of 200 keV/u, C^{6+} ions with the energy of 40 MeV/u or protons with the energy of 500 keV/u, and C^{6+} ions with the energy of 80 MeV/u or protons with the energy of 1 MeV/u, respectively [12,13]. We have confirmed that the places where H_2O^+ ions are produced depend on only the cross sections and are independent of the ion energies. The numbers of the H_2O^+ ions produced here are almost the same as the values estimated by the mean path between ionization events shown in Sec. I. However, the intervals between the H_2O^+ ions are greatly dispersed for each track, and this dispersion influences the composite electric field.

Figure 3 shows the composite electric fields formed from the irradiations of ions on the x axis as a function of x. The x axis is randomly chosen in one direction, which is perpendicular to the track of the incidental ion from the center of the target. The composite electric fields formed from the ion-impact ionization cross section of 1.5×10^{-15} cm^2 are about three, five, and ten times as large as those of 4×10^{-16}, 2×10^{-16}, and 10^{-16} cm^2, respectively. It should be noted that we show the results averaged over 100 cases where the H_2O molecules are in various positions and various electron energies are emitted from H_2O in Figs. 3–5.

B. Trap of electrons

Figures 4(a)–4(c) show the relationship of the ratios of the seed electron number with the distance from the track for (a) the C^{6+} ions with the energy of 3 MeV/u (the ion-impact ionization cross sections of 1.5×10^{-15} cm^2), (b) the proton with the energy of 200 keV/u (the ion-impact ionization cross sections of 4×10^{-16} cm^2), and (c) the proton with the energy of 1 MeV/u (the ion-impact ionization cross sections of 10^{-16} cm^2) as a function of time, respectively. Here, the seed electron [we designate this as $e^-(s1)$] is defined as those electrons produced from the process of $[A^{z+} + H_2O \rightarrow A^{z+} + H_2O^+ + e^-(s1)]$, where A^{z+} is the C^{6+} ion or the proton. In these figures, we divide these distances into six regions, that is, 0 to 1, 1 to 2, 2 to 3, 3 to 4, 4 to 5 nm, and larger than 5 nm. The ratios of the electrons trapped within the distance of 5 nm (1 nm) from the track are about 70% (45%), 50% (25%), and 25% (10%) for the C^{6+} ions with the energy of 3 MeV/u,

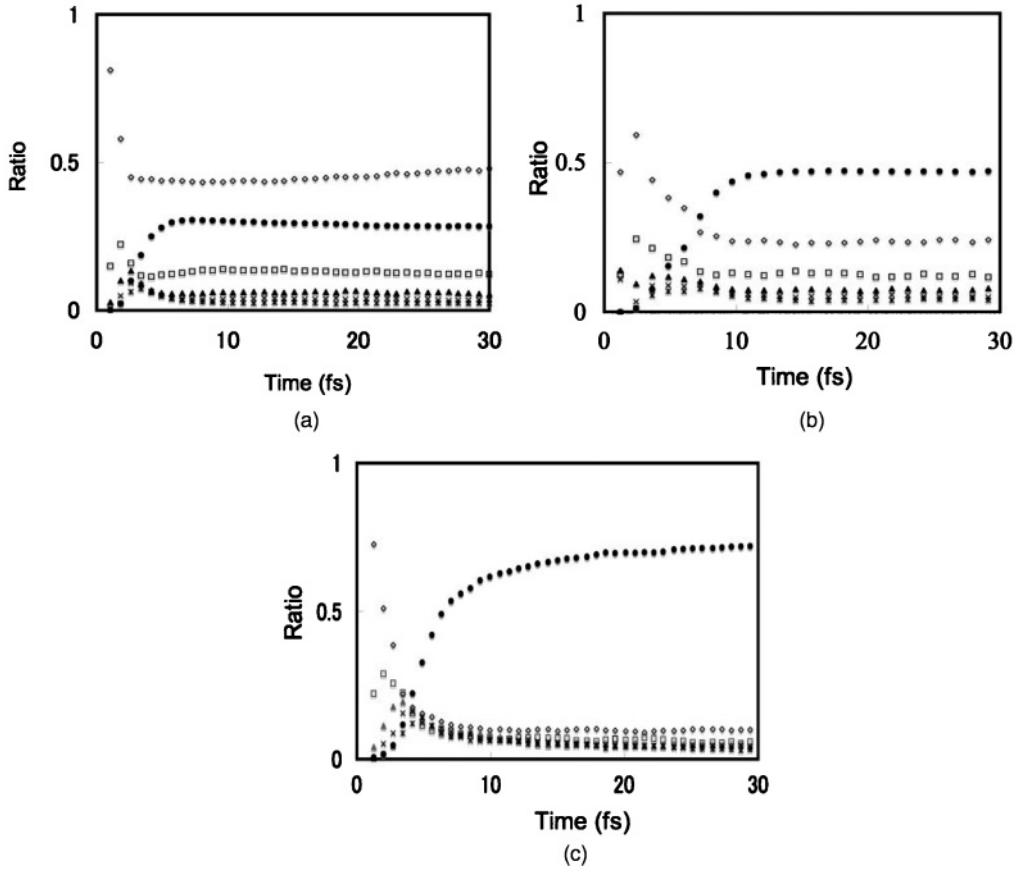

FIG. 4. The relationship of the ratios of the seed electron number with the distance from the track of (a) the C^{6+} ions with the energy of 3 MeV/u (the impact ionization cross sections of 1.5×10^{-15} cm^2), (b) the proton with the energy of 200 keV/u (the impact ionization cross sections of 4×10^{-16} cm^2), (c) the proton with the energy of 1 MeV/u (the impact ionization cross sections of 10^{-16} cm^2): The distances are ◇, 0 to 1 nm; □, 1 to 2 nm; ▲, 2 to 3 nm; ×: 3 to 4 nm; ∗, 4 to 5 nm, ● over 5 nm.

the proton with the energy of 200 keV/u, and the proton with the energy of 1 MeV/u, respectively [see Figs. 4(a)–4(c)]. We have found that there is a big difference in the numbers of electrons trapped in the composite electric field between the ion-impact ionization cross sections of 1.5×10^{-15} cm^2 (in the case of C^{6+} ions with the energy of 3 MeV/u) and 10^{-16} cm^2 (in the case of protons with the energy of 1 MeV/u).

C. Number of the electrons produced here

The number and the initial energy of electrons produced here play an important role in the DNA damage. Figure 5 shows the electron numbers of (i) seed electrons [$e^-(s1)$], (ii) secondary electrons [we designate this as $e^-(s2)$], (iii) tertiary electrons [$e^-(t)$], and (iv) electrons emitted from the excited states of H_2O through electron-impact ionization [$e^-(fe)$] as a function of time. The incident ion and its energy are the C^{6+} ion and 3 MeV/u, respectively (The incident ion-impact ionization cross section is 1.5×10^{-15} cm^2). Here, we define $e^-(s2)$, $e^-(t)$, and $e^-(fe)$ as the electrons produced from the processes [e^- $(s1) + H_2O \rightarrow e^-$ $(s\ 1) + H_2O^+ + e^-$ $(s2)$], $\{[\ e^-(s2, \text{or } t, \text{or } fe)] + H_2O \rightarrow [e^-(s2, \text{or } t, \text{or } fe)] + H_2O^+ + e^-(t)\}$, and $\{[\ e^-(s1, s2, \text{or } t, \text{or } fe)] + H_2O^* \rightarrow [e^-(s1, s2, \text{or } t, \text{or } fe)] + H_2O^+ + e^-(fe)\}$, respectively. As mentioned before, few $e^-(t)$ and $e^-(fe)$ are produced by excluding the composite electric field. Until 100 fs after the ion enters into the target, the numbers of $e^-(s1)$ and $e^-(s2)$ dominate. However, the numbers of $e^-(t)$ and $e^-(fe)$ increase rapidly after 50 fs, and their numbers become comparable to those of $e^-(s1)$ or $e^-(s2)$ around 120 fs. Around 100 fs, the electron density and ion density within 1 nm from the track of the incident ion become so high that the recombination processes may start [32], that is, the number of the electrons decreases or retains a constant value. However, the recombination processes as well as the remaining electrons may produce electronic excited states of H_2O, and the excited states of H_2O are dissociated into OH, which gives rise to the DNA damage [9,10].

D. Initial electron energies

Figure 6 shows the electron distributions of $[e^-(s1) + e^-(s2)]$, $e^-(t)$, and $e^-(fe)$ as a function of the initial electron energy. We treat the same incident ion and ion energy as those in Fig. 5. The electron distributions of $[e^-(s1) + e^-(s2)]$ calculated by excluding the electric fields are also shown (we designate this as $[e^-(s1') + e^-(s2')]$). In order to study the effect of the composite electric fields, we compare the electron distribution of $e^-(t)$ and $e^-(fe)$ with that of $[e^-(s1') +$

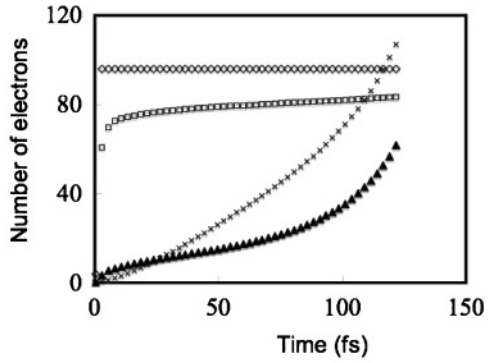

FIG. 5. The electron number of (i) seed electrons $e^-(s1)$ (◇), (ii) secondary electrons $e^-(s2)$ (□), (iii) tertiary electrons $e^-(t)$ (▲), and (iv) electrons produced from electron-impact ionization from the excited states of H_2O $e^-(fe)$ (×) as a function of time. The incident ion and its energy (the impact ionization cross sections) are C^{6+} ions and 3 MeV/u (1.5×10^{-15} cm^2), respectively.

$e^-(s2')$]. We have found that the initial energies of $e^-(fe)$ and $e^-(t)$ are in the range of a few eV and 15 to 18 eV, respectively, on the other hand, most of the initial energies of $[e^-(s1') + e^-(s2')]$ range from a few eV to 15 eV. Electrons with energies lower than 10 eV, which corresponds to the excitation energy of H_2O, contribute significantly to DNA damage through the dissociative electron attachment to H_2O, which produces OH [33], and DNA, which produce DNA damage [34]. Namely, these electrons eventually contribute only once to the production of OH or DNA damage. On the other hand, electrons with energies between 10 and 20 eV can change the states of atoms to excited or ionized ones, and their energies become lower than 10 eV. These electrons can contribute twice to the production of OH or DNA damage. The number of $[e^-(s1') + e^-(s2')]$ is almost the same as that of $[e^-(fe) + e^-(t)]$ around 100 fs, and the number of $[e^-(s1') + e^-(s2')]$, with the energy greater than 10 eV, is about half as large as that of $e^-(t)$. There is a much smaller number of electrons with initial energies higher than 20 eV for $[e^-(s1') + e^-(s2')]$. They leave the track of the incident ion and produce

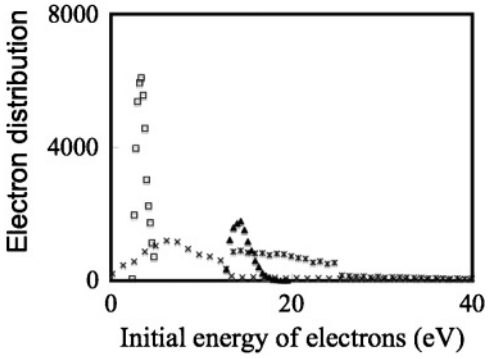

FIG. 6. The electron distribution of $[e^-(s1) + e^-(s2)]$ (∗), $[e^-(s1') + e^-(s2')]$ (×), $e^-(fe)$ (□), and $e^-(t)$ (▲) as a function of initial electron energy. The incident ion and its energy (the impact ionization cross sections) are C^{6+} ions and 3 MeV/u (1.5×10^{-15} cm^2), respectively.

OH or DNA damage at places far from the track. On the other hand, electrons with initial energy lower than 20 eV produce them near the track. Therefore, we judge that $[e^-(fe) + e^-(t)]$ contribute more significantly than $[e^-(s1') + e^-(s2')]$ to the DNA damage, in particular, cluster DNA damage, which is apt to be produced near the track and may play an important role in RBE [9,10]. In the case of the irradiation of protons, none of $e^-(t)$ and $e^-(fe)$ are created (not shown here). In this case, this may come from the fact that electron energies are lower than the excitation and ionization energies of H_2O because the acceleration due to the composite electric field is weaker.

V. CONCLUSIONS

We incorporate the effect of the composite electric fields of molecular ions as a simulation tool for the DNA damage due to the heavy-ion irradiation. Here, the molecular ions are produced from the incident ion-impact ionization processes. We calculate (i) the number and the initial energies of electrons produced from the impact ionization processes of the incident ion and electrons and (ii) the movement of the electrons in the composite electric fields. The composite electric fields due to the irradiation of a C^{6+} ion with energies of a few MeV/u increase the frequency of the electron-impact ionization processes near the track of the incident ion. This leads to an increase in the number of electrons near the track. Therefore, these composite electric fields may promote the DNA damage, in particular, cluster DNA damage. The models given in this paper are also important in atomic and molecular elementary processes in electric fields and in the production of plasmas due to heavy-ion irradiation.

The effect of the composite electric fields becomes more important as the charge of an incident ion becomes higher. This means that the study of composite electric fields may be necessary in the research of human bodies or semiconductors [3] in the space environment, where there are a lot of highly charged ions. We will study heavier incident ions, such as Fe^{26+} ions and a target of semiconductors in the future. We will also treat the ion-impact inner-shell ionization of atoms or molecules in the target. Although the cross sections of inner-shell ionization processes by incident ion impact are much smaller than those of the outer-shell ionization, the inner-shell ionization produced energetic secondary electrons and Auger electrons, which may promote DNA damage.

ACKNOWLEDGMENTS

We wish to thank Y. Iriki (Kyoto University), Professors H. Tsuchida and A. Ito (Kyoto University), T. Kenmotsu and M. Wada (Doshisha University), T. Tajima (Munich University), Dr. K. Akamatsu, Dr. T. Kai, Dr. H. Murakami, Dr. M. Kishimoto, Dr. M. Kado, Dr. N. Shikazono, Dr. J. Koga, Dr. M. Yamagiwa, Dr. R. Watanabe, Dr. K. Fujii, Dr. A. Yokoya, Dr. K. Saito, and Dr. A. Tanaka (JAEA) for their useful discussions.

[1] E. A. Blakely and A. Kronenberg, Radiat. Res. **150**, S126 (1998).
[2] Y. Kobayashi, T. Funayama, S. Wada, M. Taguchi, and H. Watanabe, Nucl. Instrum. Methods Phys. Res. B **210**, 308 (2003).
[3] J. S. Laird, T. Hirao, S. Onoda, and H. Itoh, J. Appl. Phys. **98**, 013530 (2005).
[4] K. Motohashi, S. Tsurubuchi, and A. Koukitu, Nucl. Instrum. Methods Phys. Res. B **232**, 254 (2005).
[5] K. Awazu, S. Ishii, K. Shima, S. Roorda, and J. L. Brebner, Phys. Rev. B **62**, 3689 (2000).
[6] R. R. Wilson, Radiology **47**, 487 (1946).
[7] M. Murakami *et al*., AIP Conf. Proc. **1024**, 275 (2008).
[8] A. Yogo *et al*., Appl. Phys. Lett. **94**, 181502 (2009).
[9] J. F. Ward, Int. J. Radiat. Biol. **66**, 427 (1994).
[10] D. T. Goodhead, Int. J. Radiat. Biol. **65**, 7 (1994).
[11] Y. Sato *et al*., AIP Conf. Proc. **771**, 128 (2005).
[12] C. D. Cappello, C. Champion, O. Boudrioua, H. Lekadir, Y. Sato, and D. Ohsawa, Nucl. Instrum. Methods Phys. Res. B **267**, 781 (2009).
[13] S. Uehara, L. H. Toburen, W. E. Wilson, D. T. Goodhead, and H. Nikjoo, Radiat. Phys. Chem. **59**, 1 (2000).
[14] S. P. Hau-Riege, R. A. London, H. N. Chapman, A. Szoke, and N. Timneanu, Phys. Rev. Lett. **98**, 198302 (2007).
[15] O. J. Orient and S. K. Srivastava, J. Phys. B **20**, 3923 (1987).
[16] H. P. Pritchard, V. McKoy, and M. A. P. Lima, Phys. Rev. A **41**, 546 (1990).
[17] K. Moribayashi, J. Phys.: Conf. Ser. **58**, 192 (2007).
[18] S. Uehara and H. Nikjoo, J. Phys. Chem. B **106**, 11051 (2002).
[19] R. K. Janev, L. P. Presnyakov, and V. P. Shevelko, *Physic of Highly Charged Ions*, Vol. 13 Springer Series in Electrophysics (Springer-Verlag, Berlin, 1985), Chaps. 7 and 8.
[20] T. V. Goffe, M. B. Shah, and H. B. Gilbody, J. Phys. B **12**, 3763 (1979).
[21] Z. Jurek, G. Faigel, and M. Tegze, Eur. Phys. J. D **29**, 217 (2004).
[22] K. Moribayashi, Phys. Rev. A **80**, 025403 (2009).
[23] K. Moribayashi, J. Phys. B **43**, 165602 (2010).
[24] K. Moribayashi, Prog. Nucl. Sci. Technol. (to be published).
[25] K. Moribayashi, A. Sasaki, and T. Tajima, Phys. Rev. A **58**, 2007 (1998).
[26] K. Moribayashi, A. Sasaki, and T. Tajima, Phys. Rev. A **59**, 2732 (1999).
[27] T. Kai, Phys. Rev. A **81**, 023201 (2010).
[28] M. E. Rudd, Y. K. Kim, D. H. Madison, and T. J. Gay, Rev. Mod. Phys. **64**, 441 (1992).
[29] S. Nakazaki, M. Nakashima, H. Takebe and K. Takayanagi, J. Phys. Soc. Jpn. **60**, 1565 (1991).
[30] T. Nishimura and Y. Itikawa, J. Phys. B **28**, 1995 (1995).
[31] W. Lotz, Z. Phys. **232**, 101 (1970).
[32] T. Fujimoto, *Plasma Spectroscopy*, Vol. 123 International series of monographs on physics, edited by J. Birman *et al*. (Clarendon / Oxford Science, Oxford, 2004), Chap. 5.
[33] P. Rawat, V. S. Prabhudesai, G. Aravind, M. A. Rahman, and E. Krishnakumar, J. Phys. B **40**, 4625 (2007).
[34] K. Aflatooni, A. M. Scheer, and P. D. Burrow, J. Chem. Phys. **125**, 054301 (2006).